Li-Fi and Wi-Fi with Common Backhaul: Coordination and Resource Allocation

Vasilis K. Papanikolaou*, Panagiotis P. Bamidis*, Panagiotis D. Diamantoulakis*, George K. Karagiannidis*
*Department of Electrical and Computer Engineering, Aristotle University of Thessaloniki, GR-54124 Thessaloniki, Greece
e-mails: {vpapanikk, pmpamidis, padiaman, geokarag}@auth.gr

***Abstract*—Visible light communication (VLC) -also known as light fidelity (Li-Fi)- networks will play an important role in the near future, since they will provide full coverage and improved data rates for indoor wireless applications. In this paper, the coexistence of Li-Fi and Wi-Fi networks is investigated for the multi-user scenario, under the practical assumption that both of them are served by the same backhaul network (e.g., optical fiber). More specifically, we study the resource allocation and coordination problems by maximizing the proportional fairness of all users. To do so, we formulate and solve an optimization problem for the power allocation of the hybrid Li-Fi/Wi-Fi scenario, under the constraint of the common backhaul. Computer simulation results are provided to illustrate the effectiveness of the proposed analysis.**

I. Introduction

Wireless communications are a staple part of everyday life and are dominated by the use of radio frequencies (RF). Incorporating Internet-of-Things (IoT) applications with current wireless technologies is predicted to lead to a looming "spectrum crunch", due to the huge increase in data traffic that current network technologies will have to accommodate. With the release of IEEE 802.11ad standard, which also incorporates mmWave frequencies, it is natural to assume that a solution to the aforementioned problem lies in the use of a different region of the electromagnetic spectrum. This assumption has led to the introduction of visible light communications (VLC). VLC has emerged in very recent years as a promising solution for overcoming issues that contemplate standard RF wireless technologies [1]–[5]. By exploiting a vast, unregulated and, free region of the electromagnetic spectrum, VLC provides the necessary bandwidth to counter the ever more crowding in the radio spectrum, while remaining unwavered by electromagnetic interference from the current wireless solutions. This is especially attractive for RF-sensitive applications, where electromagnetic radiation can be considered harmful, such as in hospitals. Furthermore, VLC makes use of energy-efficient LED-based transmitters that also provide illumination to the spaces that are used [3]. Also, the data rates reported for VLC networking are much higher than those achieved by Wi-Fi in the indoor scenario, while it also offers increased physical security since light does not propagate through walls [6]–[9].

However, the main drawback of the VLC networking solution, also referred to as light fidelity (Li-Fi), is its limited coverage capabilities, especially in the indoor scenario, where optical radiation can easily be blocked and the optical link can easily be interrupted, due to the movement or rotation of the receiver. On the contrary, the RF-based Wi-Fi can achieve ubiquitous coverage. Consequently, the heterogeneous networking of Li-Fi and Wi-Fi (VLC and RF) could take advantage of both technologies so that hybrid systems with coordinated use of both Wi-Fi and Li-Fi can be used to fully exploit the system capacity, while ensuring access to all locations.

In coordinated Heterogeneous Networks (HetNets), such as the hybrid Li-Fi/Wi-Fi, there are numerous challenges to overcome, in order to ensure fairness to all users. However, in this particular Li-Fi/Wi-Fi HetNet, there is the need for new coordination and resource allocation schemes in order to optimize the load balancing (LB) of the network. Specifically, due to Li-Fi's limited coverage there is the need for effective handover schemes between Li-Fi and Wi-Fi to ensure full time connectivity. This is usually formulated as an optimization problem of power and rate allocation in order to ensure user fairness. The constraints are based on the limitations of both the Wi-Fi and the Li-Fi Access Points (APs), concerning, primarily, the power consumption of the APs. While the LB schemes and the handover schemes are well-explored [10], [11], the effect of a limitation concerning the backhaul network is much less so. In [12], the use of power line communications (PLC) is considered as a backhaul network for the Li-Fi part, since it can be cost-effective. Furthermore, the case that the backhaul is implemented with an optical fiber is also considered in the current state-of-the-art [13]. While PLC offers many advantages, primarily on how easily it can be incorporated (Plug & Play), it suffers from frequency selective channel gain and impulse noise. In a realistic scenario, both Wi-Fi and Li-Fi will share the same backhaul infrastructure. This is even more reasonable when we consider that a common subscription line will be available from the network provider for both of them. To the best of the authors' knowledge, this subject has not been investigated in the existing literature.

To this end, in this paper, we investigate the power allocation problem of a multi-user coordinated Li-Fi/Wi-Fi network, under the practical assumption that both Li-Fi and Wi-Fi share the same backhaul network. In such a network the standard sum rate optimization can lead to Li-Fi accumulating the available rate from the backhaul, which, in turn, might considerably degrade the provided quality of service (QoS) to Wi-Fi users. This calls for the development of an appropriate optimization framework to guarantee proportional fairness, which is the main challenge addressed in this work. More

978-1-5386-1734-2/18/$31.00 ©2018 IEEE

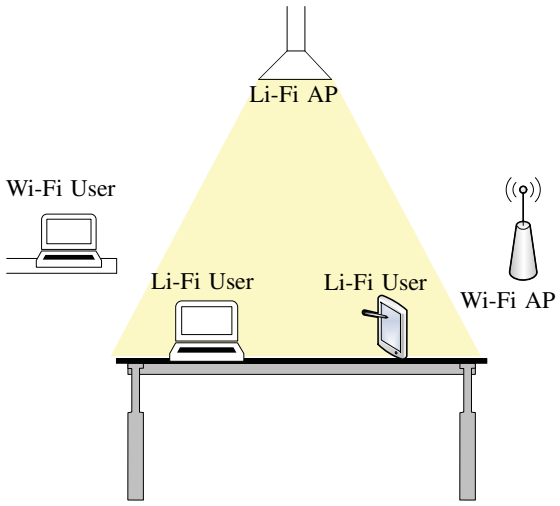

Fig. 1. System Model

specifically, we propose the use of rate and power allocation algorithms, to ensure that the proportional fairness among all users is maximized. We formulate and, solve an optimization problem for the power allocation of the hybrid Li-Fi/Wi-Fi scenario, under the constraint of the common backhaul. Even though, this work focuses on the downlink scenario, the analysis can be easily generalized and include the uplink case too. Finally, through computer simulations, we show that for the case of low backhaul capacity, both the Li-Fi and the Wi-Fi users can fairly share similar data rates. However, if the backhaul network provides a large enough capacity, the Li-Fi users can take advantage and reach even higher data rates, while the Wi-Fi subsystem reaches a floor.

II. System and Channel Model

We consider the downlink transmission of a coordinated Li-Fi/Wi-Fi network, consisting of one VLC access point (AP), one RF AP, and multiple users, as in Figs. 1 and 2. We assume two users groups, with $\mathcal{N} = \{1, ..., n, ...N\}$ and $\mathcal{M} = \{1, ..., m, ...M\}$ served by the VLC and RF AP, respectively. We further assume that the two networks share the same backhaul (e.g., optical fiber), the capacity of which is fixed and equal to C_0, as it is illustrated in Fig. 2. Also, it is assumed that all mobile nodes are equipped with single antennas/optical receivers and each user utilizes solely an orthogonal communication channel, with B, t and w, τ being its bandwidth and timeslot duration for the VLC and RF communication system, respectively. For presentantion clarity, we assume that time division multiple access (TDMA) and orthogonal frequency division multiple access (OFDMA) are used for the VLC and RF system, respectively [7], [8]. However, the following analysis is directly applicable to different multiple access schemes. Note that the use of TDMA for VLC has been considered in the literature [14], because of its low complexity. Thus, B corresponds to the the bandwidth of the VLC system, $t = \frac{T}{N}$, $w = \frac{W}{M}$, and $\tau = T$, where T is the transmission frame period.

A. Optical Wireless Transmission

1) Channel Model: The channel power gain is given by [15], [16]

$$h_n = \frac{L_r}{d_n^2} r_0(\varphi) T_s(\psi) g(\psi) \cos(\psi), \tag{1}$$

where L_r is the physical area of the photo-detector, d is the transmission distance from the LED to the illuminated surface of the photo-detector, $T_s(\psi)$ is the gain of the optical filter and $g(\psi)$ represents the gain of the optical concentrator, given by [15], [17]

$$g(\psi) = \begin{cases} \frac{\rho^2}{\sin^2(\Psi_{\text{fov}})}, & 0 \le \psi \le \Psi_{\text{fov}}, \\ 0, & \psi > \Psi_{\text{fov}}. \end{cases} \tag{2}$$

with ρ and Ψ_{fov} being the refractive index and FOV, respectively. Also in (1), $r_0(\varphi)$ is the Lambertian radiant intensity of the LED, given by

$$r_0(\varphi) = \frac{\xi + 1}{2\pi} \cos^{\xi} \varphi, \tag{3}$$

where φ is the irradiance angle, ψ is the incidence angle, and

$$\xi = -\frac{1}{\log_2 \cos(\Phi_{1/2})}, \tag{4}$$

with $\Phi_{1/2}$ being the semi-angle at half luminance.

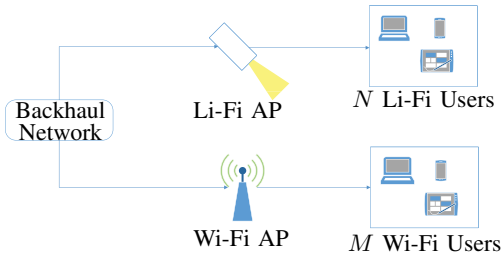

Fig. 2. Li-Fi and Wi-Fi sharing the same backhaul network

2) Achievable Rate: We express the achievable rate by the n-th user, using a lower bound of the capacity given by [18]

$$R_n^{[\text{VLC}]} = tB \log_2 \left(1 + \frac{e}{2\pi} \gamma_n^{[\text{VLC}]}\right), \tag{5}$$

where B is the bandwidth of the VLC system, t is the the transmission timeslot, and $\gamma_n^{[\text{VLC}]}$ is the received SNR, which is written as follows [10],

$$\gamma_n^{[\text{VLC}]} = \frac{(\eta h_n P_n)^2}{\sigma^2}. \tag{6}$$

In (6), P_n is the transmitted optical power to the n-th user, σ^2 is the noise power and, η denotes the photodetector's responsivity. Note that, the achievable rate of the VLC system is also limited by the average optical power (lighting constraint), i.e.,

$$\sum_{n=1}^{N} P_n \le N P_{\text{av}}. \tag{7}$$

B. RF Transmission

The path loss factor of the link between the RF AP to user m is denoted by L_m, while the channel coefficient is given by the complex random variable $h_m \sim \mathcal{CN}(0,1)$. The achievable rate can be written as

$$R_m^{[\mathrm{RF}]} = Tw \log_2 \left(1 + \frac{L_m h_m^2 p_m}{N_0 w}\right), \tag{8}$$

where N_0 is the power spectral density of the white noise for the RF system. Also, the following constraint needs to be satisfied

$$\sum_{m=1}^{M} p_m \leq p_{\max}. \tag{9}$$

III. Rate and Power Allocation

The main challenge in multi-user networks, which consist of users with different characteristics, is the trade-off between fairness and performance. In these cases, the proportional fairness, defined as the sum–log–rate, is the most approporiate metric to optimize [10], [19]. In what follows, we aim to maximize the proportional fairness, [20], while also achieving a balance between the rates achieved by each system, i.e., the Li-Fi and the Wi-Fi, by using the weight $0 \leq \alpha \leq 1$. The corresponding optimization problem can be written as follows

$$\begin{aligned} \underset{\mathbf{P},\mathbf{p}}{\mathbf{max}} \quad & \alpha \textstyle\sum_{n=1}^{N} \log(R_n^{[\mathrm{VLC}]}) + (1-\alpha) \sum_{m=1}^{M} \log(R_m^{[\mathrm{RF}]}) \\ \mathbf{s.t.} \quad & \mathrm{C}_1 : \textstyle\sum_{n=1}^{N} R_n^{[\mathrm{VLC}]} + \sum_{m=1}^{M} R_m^{[\mathrm{RF}]} \leq C_0, \\ & \mathrm{C}_2 : \textstyle\sum_{n=1}^{N} P_n \leq N P_{\mathrm{av}}, \\ & \mathrm{C}_3 : \textstyle\sum_{m=1}^{M} p_m \leq p_{\max}. \end{aligned} \tag{10}$$

The first constraint ensures that the total data rate of both Li-Fi and Wi-Fi is less than the capacity of the backhaul network. Moreover, the maximum allowable power consumption of both systems are dictated by the physical limitations of the APs. These conditions are realized with constraints 2 and 3. It is noted that the optimization problem (10) is non-convex because of the term related to the VLC rate in the objective function and C_1, particularly, because of the squared term of the n-th user's power. Also, the RF related term in C_1 is required to be convex, while it's concave. Therefore the complexity to solve it is high, mainly due to the relation of the rates with the power allocation variables. It is important to prove, that the problem in (10) can be transformed to a convex one, and, as such, the process to find a global maximum can be solved in polynomial time, in order to derive a tractable power allocation algorithm to ensure proportional fairness.

Lemma 1: The problem in (10) can be formulated as a convex one.

Proof: First, the objective function needs to be transformed into a concave one. To this end, we use two auxiliary variables, r_n^{VLC}, $\forall n \in \mathcal{N}$ and r_m^{RF}, $\forall m \in \mathcal{M}$, respectively, such that

$$r_n^{\mathrm{VLC}} \leq R_n^{[\mathrm{VLC}]}, \tag{11}$$

$$r_m^{\mathrm{RF}} \leq R_m^{[\mathrm{RF}]}. \tag{12}$$

Furthermore, by using

$$P_n = e^{\tilde{P}_n}, \forall n \in \mathcal{N} \text{ and } p_m = e^{\tilde{p}_m}, \forall m \in \mathcal{M}, \tag{13}$$

C_2 and C_3 of (10) are convex because they are both sum of exponentials. Then, the problem of (10) is formulated as

$$\begin{aligned} \underset{\tilde{\mathbf{P}},\tilde{\mathbf{p}},\mathbf{r}^{\mathrm{VLC}},\mathbf{r}^{\mathrm{RF}}}{\mathbf{max}} \quad & \alpha \textstyle\sum_{n=1}^{N} \log(r_n^{\mathrm{VLC}}) + (1-\alpha) \sum_{m=1}^{M} \log(r_m^{\mathrm{RF}}) \\ \mathbf{s.t.} \quad & \mathrm{C}_1 : \textstyle\sum_{n=1}^{N} r_n^{\mathrm{VLC}} + \sum_{m=1}^{M} r_m^{\mathrm{RF}} \leq C_0, \\ & \mathrm{C}_2 : \textstyle\sum_{n=1}^{N} e^{\tilde{P}_n} \leq N P_{\mathrm{av}}, \\ & \mathrm{C}_3 : \textstyle\sum_{m=1}^{M} e^{\tilde{p}_m} \leq p_{\max}, \\ & \mathrm{C}_4 : R_n^{[\mathrm{VLC}]} \geq r_n^{\mathrm{VLC}}, \forall n \in \mathcal{N}, \\ & \mathrm{C}_5 : R_m^{[\mathrm{RF}]} \geq r_m^{\mathrm{RF}}, \forall m \in \mathcal{M}. \end{aligned} \tag{14}$$

The objective function of (14) is now concave because it is the sum of logarithms. However, due to the constraints, introduced with the use of (11) and (12), i.e., C_4 and C_5, problem (14) remains non-convex and we cannot end our proof here. Regarding C_4, by setting $G^2 = \frac{e\eta^2 h_n^2}{2\pi\sigma^2}$ and using (13), it can now be written as

$$Bt \log_2 \left(1 + G^2 P_n^2\right) \geq r_n^{\mathrm{VLC}} \Leftrightarrow \frac{1}{G^2}\left(2^{\frac{r_n^{\mathrm{VLC}}}{Bt}} - 1\right) \leq e^{2\tilde{P}_n}, \tag{15}$$

which, in turn, can be rewritten as

$$\frac{1}{2}\log\left(2^{\frac{r_n^{\mathrm{VLC}}}{Bt}} - 1\right) - \frac{1}{2}\log G^2 - \tilde{P}_n \leq 0. \tag{16}$$

With its current form, we just need to prove that the left part of (16) is convex. Thus, we use the following transformation

$$r_n^{\mathrm{VLC}} = \exp\left(\tilde{r}_n^{\mathrm{VLC}}\right), \qquad \forall n \in \mathcal{N}, \tag{17}$$

$$r_m^{\mathrm{RF}} = \exp\left(\tilde{r}_m^{\mathrm{RF}}\right), \qquad \forall m \in \mathcal{M}, \tag{18}$$

and we will continue our proof by proving the convexity of the resulting functions. We have to prove the convexity using the Hessian matrix, rather than just the second derivative, since constraint 4 depends on two of the problem's variables. Using (17), we get

$$f = \frac{1}{2}\log\left(2^{\frac{1}{Bt}\exp\left(\tilde{r}_n^{\mathrm{VLC}}\right)} - 1\right) - \frac{1}{2}\log G^2 - \tilde{P}_n. \tag{19}$$

The Hessian Matrix of function $f(\tilde{r}_n^{\mathrm{VLC}}, \tilde{P}_n)$ is defined as

$$\mathbf{H} = \begin{bmatrix} \frac{\partial^2 f}{\partial \tilde{r}_n^{\mathrm{VLC}^2}} & \frac{\partial^2 f}{\partial x r_n^{\mathrm{VLC}} \partial \tilde{P}_n} \\ \frac{\partial^2 f}{\partial P_n \partial \tilde{r}_n^{\mathrm{VLC}}} & \frac{\partial^2 f}{\partial P_n^2} \end{bmatrix}. \tag{20}$$

We evaluate the following partial derivatives to get the Hessian matrix,

$$\frac{\partial^2 f}{\partial \tilde{P}_n^2} = \frac{\partial^2 f}{\partial \tilde{r}_n^{\mathrm{VLC}} \partial \tilde{P}_n} = \frac{\partial^2 f}{\partial \tilde{P}_n \partial \tilde{r}_n^{\mathrm{VLC}}} = 0, \tag{21}$$

$$\frac{\partial^2 f}{\partial \tilde{r}_n^{\mathrm{VLC}^2}} = \frac{1}{2}\frac{2^z \log(2)\left(2^z - z\log(2) - 1\right)}{(2^z - 1)^2}, \tag{22}$$

where z is defined by $z = \frac{1}{Bt}\exp\left(\tilde{r}_n^{\mathrm{VLC}}\right)$. Considering that $y = 2^z - z\log(2) - 1$ is an increasing function with respect

to z and when $z \to 0$, $y \to 0$, it is shown that $\frac{\partial^2 f}{\partial \tilde{r}_n^{\mathrm{VLC}2}} \geq 0$. Then, it's obvious that the Hessian matrix of f is positive semi-definite, due to the matrix being diagonal with non-negative terms, so its eigenvalues are non-negative. Consequently f is a convex function.

Next, we follow the same approach for C_5. After similar calculations as before we get

$$g = \log\left(2^{\frac{\exp(\tilde{r}_m)}{Tw}} - 1\right) - \log A^2 - \tilde{p}_m, \tag{23}$$

where $A = \frac{L_m h_m^2}{w N_0}$. By the definition of the parameters and the analysis for the fourth constraint, it is obvious that the Hessian matrix of (23) is positive semi-definite, as such, g is convex.

Thus, convexity has been proved for the optimization problem, with all the required transformations. ∎

As such, the equivalent convex problem can be formulated as follows,

$$\begin{aligned}
\underset{\tilde{\mathbf{P}},\tilde{\mathbf{p}},\tilde{\mathbf{r}}^{\mathrm{VLC}},\tilde{\mathbf{r}}^{\mathrm{RF}}}{\mathbf{max}} \quad & \alpha \textstyle\sum_{n=1}^{N} \tilde{r}_n^{\mathrm{VLC}} + (1-\alpha) \sum_{m=1}^{M} \tilde{r}_m^{\mathrm{RF}} \\
\textbf{s.t.} \quad & \mathrm{C}_1 : \textstyle\sum_{n=1}^{N} \exp\left(\tilde{r}_n^{\mathrm{VLC}}\right) + \\
& \quad \textstyle\sum_{m=1}^{M} \exp\left(\tilde{r}_m^{\mathrm{RF}}\right) \leq C_0, \\
& \mathrm{C}_2 : \textstyle\sum_{n=1}^{N} e^{\tilde{P}_n} \leq N P_{\mathrm{av}}, \\
& \mathrm{C}_3 : \textstyle\sum_{m=1}^{M} e^{\tilde{p}_m} \leq p_{\max}, \\
& \mathrm{C}_4 : \tilde{P}_n - \tfrac{1}{2}\log\left(\frac{2^{\exp(\tilde{r}_n^{\mathrm{VLC}})/(Bt)}-1}{G^2}\right) \geq 0, \\
& \quad \forall n \in \mathcal{N}, \\
& \mathrm{C}_5 : \tilde{p}_m - \log\left(\frac{2^{\left(\exp(\tilde{r}_m^{\mathrm{RF}})\right)/(Tw)}-1}{A^2}\right) \geq 0, \\
& \quad \forall m \in \mathcal{M}.
\end{aligned} \tag{24}$$

Once again, C_1 represents the limited capacity offered from the shared backhaul network, while C_2 and C_3 include the hardware limitations of the APs for power consumption. C_4 and C_5 are extra constraints that are needed because of the way that we introduced the auxiliary variables in equations (11) and (12), and, also, they contain information about the rates of the Li-Fi and the Wi-Fi subsystems. We, then, solve (24) using the Lagrange dual decomposition method, and we obtain the Lagrangian of the problem, which is given by

$$\begin{aligned}
L = {} & \alpha \sum_{n=1}^{N} \tilde{r}_n^{\mathrm{VLC}} + (1-\alpha) \sum_{m=1}^{M} \tilde{r}_m^{\mathrm{RF}} \\
& - \lambda_1 \left(\sum_{n=1}^{N} \exp\left(\tilde{r}_n^{\mathrm{VLC}}\right) + \sum_{m=1}^{M} \exp\left(\tilde{r}_m^{\mathrm{RF}}\right) - C_0 \right) \\
& - \lambda_2 \left(\sum_{n=1}^{N} e^{\tilde{P}_n} - N P_{\mathrm{av}} \right) - \lambda_3 \left(\sum_{m=1}^{M} e^{\tilde{p}_m} - p_{\max} \right) \\
& + \sum_{n=1}^{N} \lambda_{3+n} \left(\tilde{P}_n - \frac{1}{2} \log\left(\frac{2^{\exp(\tilde{r}_n^{\mathrm{VLC}})/(Bt)} - 1}{G^2} \right) \right) \\
& + \sum_{m=1}^{M} \lambda_{3+N+m} \left(\tilde{p}_m - \log\left(\frac{2^{\left(\exp(\tilde{r}_m^{\mathrm{RF}})\right)/(Tw)} - 1}{A^2} \right) \right).
\end{aligned} \tag{25}$$

According to Karush-Kuhn-Tucker (KKT) conditions [21], the optimal values can be obtained by taking the first derivatives and setting them equal to zero. The following expressions are true $\forall n \in \mathcal{N}$ and $\forall m \in \mathcal{M}$.

$$\frac{\partial L}{\partial \tilde{P}_n} = 0 \Leftrightarrow \tilde{P}_n = \log\left(\frac{\lambda_{3+n}}{\lambda_2}\right), \tag{26}$$

$$\frac{\partial L}{\partial \tilde{p}_m} = 0 \Leftrightarrow \tilde{p}_m = \log\left(\frac{\lambda_{3+N+m}}{\lambda_3}\right), \tag{27}$$

$$\begin{aligned}
& \frac{\partial L}{\partial \tilde{r}_n^{\mathrm{VLC}}} = 0 \Leftrightarrow \lambda_1 \exp\left(\tilde{r}_n^{\mathrm{VLC}}\right) + \\
& \lambda_{3+n} \frac{\exp\left(\tilde{r}_n^{\mathrm{VLC}}\right) \log(2) 2^{\exp\left(\tilde{r}_n^{\mathrm{VLC}}\right)/(Bt)}}{2Bt\left(2^{\exp\left(\tilde{r}_n^{\mathrm{VLC}}\right)/(Bt)} - 1\right)} = \alpha,
\end{aligned} \tag{28}$$

$$\begin{aligned}
& \frac{\partial L}{\partial \tilde{r}_m^{\mathrm{RF}}} = 0 \Leftrightarrow \lambda_1 \exp\left(\tilde{r}_m^{\mathrm{RF}}\right) + \\
& \lambda_{3+N+m} \frac{\exp\left(\tilde{r}_m^{\mathrm{RF}}\right) \log(2) 2^{\exp\left(\tilde{r}_m^{\mathrm{RF}}\right)/(Tw)}}{Tw\left(2^{\exp\left(\tilde{r}_m^{\mathrm{RF}}\right)/(Tw)} - 1\right)} = 1 - \alpha.
\end{aligned} \tag{29}$$

We need to update the Lagrange multipliers so that they will be optimized. For that reason, we choose to use a subgradient algorithm, as follows

$$\begin{aligned}
\lambda_1^{(i+1)} = {} & \Bigg[\lambda_1^{(i)} + \hat{\lambda}_1^{(i)} \times \\
& \left(\sum_{n=1}^{N} \exp\left(\tilde{r}_n^{\mathrm{VLC}}\right) + \sum_{m=1}^{M} \exp\left(\tilde{r}_m^{\mathrm{RF}}\right) - C_0 \right) \Bigg]^{+},
\end{aligned} \tag{30}$$

$$\lambda_2^{(i+1)} = \left[\lambda_2^{(i)} + \hat{\lambda}_2^{(i)} \left(\sum_{n=1}^{N} e^{\tilde{P}_n} - N P_{\mathrm{av}} \right) \right]^{+}, \tag{31}$$

$$\lambda_3^{(i+1)} = \left[\lambda_3^{(i)} + \hat{\lambda}_3^{(i)} \left(\sum_{m=1}^{M} e^{\tilde{p}_m} - p_{\max} \right) \right]^{+}, \tag{32}$$

$$\begin{aligned}
\lambda_{3+n}^{(i+1)} = {} & \Big[\lambda_{3+n}^{(i)} + \hat{\lambda}_{3+n}^{(i)} \times \\
& \left(\tilde{P}_n - \frac{1}{2} \log\left(\frac{2^{\exp\left(\tilde{r}_n^{\mathrm{VLC}}\right)/(Bt)} - 1}{G^2} \right) \right) \Big]^{+}, \forall n \in \mathcal{N},
\end{aligned} \tag{33}$$

$$\begin{aligned}
\lambda_{3+N+m}^{(i+1)} = {} & \Big[\lambda_{3+N+m}^{(i)} + \hat{\lambda}_{3+N+m}^{(i)} \times \\
& \log\left(\frac{2^{\left(\exp\left(\tilde{r}_m^{\mathrm{RF}}\right)\right)/(Tw)} - 1}{A^2} \right) \Big)\Big]^{+}, \forall m \in \mathcal{M},
\end{aligned} \tag{34}$$

where $\hat{\lambda}_j^{(i)}$, $j = 1, 2, ..., 3 + N + M$ is the size of the steps at iteration i, while there is a finite number of iterations that is allowed, I_{max}. Also, note that $[x]^{+}$ means $\max(x, 0)$.

IV. Numerical Results and Simulations

In this section, Monte Carlo simulation results are presented for a system with a total of 4 users, i.e., 2 Li-Fi users and 2 Wi-Fi users, a typical scenario for a room, which is assumed to be orthogonal A 6 m × 4 m, with the Li-Fi AP located on the ceiling, in the center of the room and the Wi-Fi AP at the center of one of the walls. The locations of the users are random in order to fit the aforementioned scenario. The same

parameters as in [14] are used in the simulations. Also, for the path loss model, the following model is used from [14]

$$L(d) = L(d_0) + 10\kappa \log_{10}(d/d_0), \tag{35}$$

where $L(d_0) = 68$ dB is the reference path loss at a reference distance, $d_0 = 1$ m, and $\kappa = 1.6$ is the path loss exponent. More specifically, the impact of the backhaul capacity and α on optimal rates and power allocation is investigated.

TABLE I
PARAMETERS EXTRACTED FROM [14].

$P_{\max} = NP_{\text{av}}$	9 W	ρ	1.5
η	0.53 A/W	Ψ_{FOV}	$\pi/3$
σ^2	5×10^{-22} A^2	$\Phi_{1/2}$	$\pi/3$
B	40 MHz	p_{max}	1 W
L_r	1 cm^2	W	20 MHz
$T_s(\psi)$	1	N_0	4.002×10^{-21} A^2/W

In Fig. 3, the rates of the Li-Fi and Wi-Fi systems are plotted versus the capacity of the backhaul network, when the weight α is equal to 0.5. This, essentially, means that neither the Li-Fi nor the Wi-Fi users have priority over the data rate provided by the backhaul network. It is evident that, when the capacity is low enough, Wi-Fi can reach the same data rate as Li-Fi. So, since $\alpha = 0.5$, both subsystems share the capacity equally. However, as C_0 increases, the Wi-Fi subsystem reaches a floor, due to the saturation of the rates that it can achieve with respect to the available tranmsission power.

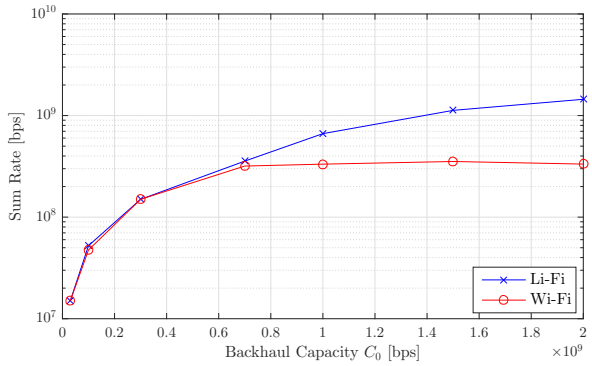

Fig. 3. Sum Rate of Li-Fi and Wi-Fi versus backhaul network capacity C_0 ($\alpha = 0.5$).

Similar conclusions can be conducted when shifting the priority to the Li-Fi system, by using values for α greater than 0.5 as In Fig. 4 where $\alpha = 0.8$. As it can be observed, the slope of sum rate for Wi-Fi decreases faster than that of Li-Fi, which also indicates that the saturation of the achievable rates of the Wi-Fi system has a prominent role on its performance. However, in this case even for lower values of the backhaul network capacity, the Wi-Fi rates appear to be lower than those of the Li-Fi. Also, here, the Li-Fi system achieves much greater data rates, than both the Wi-Fi and the Li-Fi from the previous scenario ($\alpha = 0.5$).

In Figures 5 and 6, some interesting observation can be made, regarding the impact of α on the rates of both subsystems. We observe that for the case of $\alpha = 0.5$, the Li-Fi

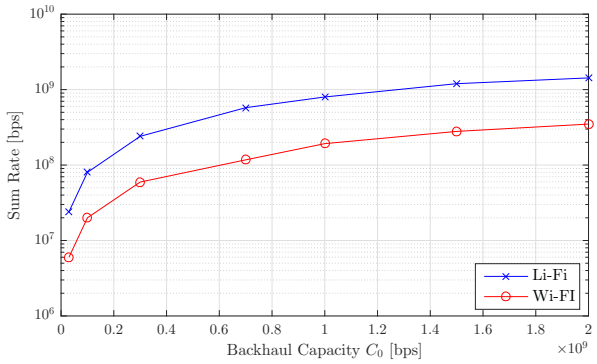

Fig. 4. Sum Rate of Li-Fi and Wi-Fi versus backhaul network capacity C_0 ($\alpha = 0.8$).

and the Wi-Fi users get very similar data rates, for a specific value of C_0. As α approaches unity, it appears that the Li-Fi users are accumulating much more of the network data rate. The purpose of the Li-Fi subsystem is to significantly increase the achievable data rate of certain users in the hybrid network. That said, depending on the use case, one can adjust the weight α to obtain the desirable QoS for each users' group. Once again, when the backhaul network provides lower data rates, the Wi-Fi can achieve data rates as fast the Li-Fi, so the only difference in the rates of these subsystems depends on the value of α.

When the backhaul offers more capacity, the way according to which the rate is allocated in the hybrid network is different. Wi-Fi cannot achieve similar rates as Li-Fi, so the Li-Fi users aggregate most of the data rate. Consequently, the curves seem unchanged with regards to α. The critical cases of $\alpha = 0$ and $\alpha = 1$ are different, since the algorithm is oblivious to the Li-Fi and Wi-Fi rates, respectively. In those cases, we observe a significant loss in rate for both subsystems.

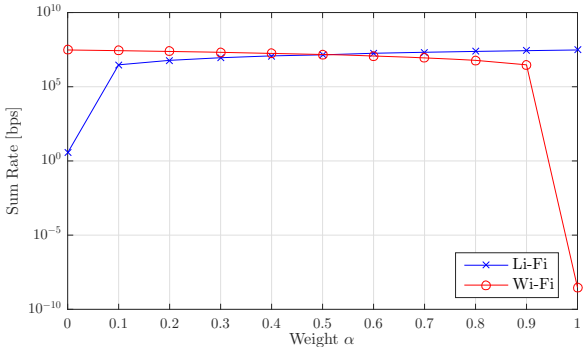

Fig. 5. Sum Rate of Li-Fi and Wi-Fi versus weight α ($C_0 = 30$ Mbps).

Next, we move to examine the power allocation for the hybrid network. The following figures show the average power per user in the Li-Fi and Wi-Fi subsystems.

In Fig. 7, we examine the power allocation of the $\alpha = 0.5$ with regards to the capacity of the backhaul network. We observe that, when the Li-Fi and the Wi-Fi users achieve the same rates, the Li-Fi actually needs less power. For higher data rates, that only Li-Fi appears to achieve, as it appears on

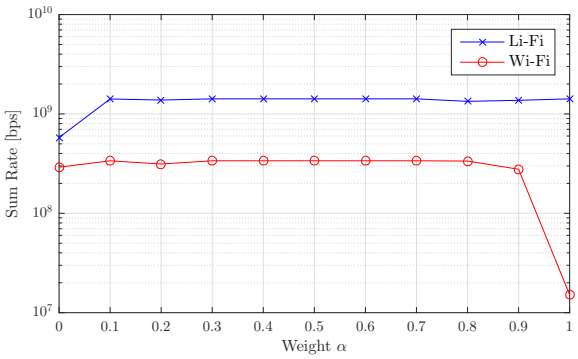

Fig. 6. Sum Rate of Li-Fi and Wi-Fi versus weight α ($C_0 = 2$ Gbps).

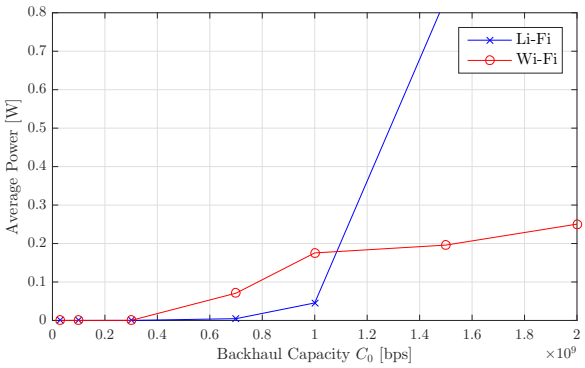

Fig. 7. Average Power per user of Li-Fi and Wi-Fi versus backhaul network capacity C_0 ($\alpha = 0.5$).

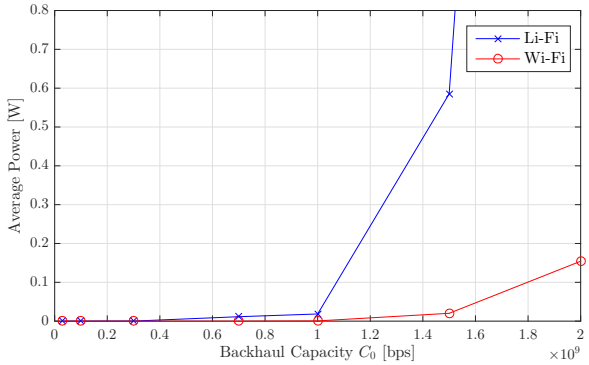

Fig. 8. Average Power per user of Li-Fi and Wi-Fi versus backhaul network capacity C_0 ($\alpha = 0.8$).

Fig. 3, the power the Li-Fi AP consumes starts to exceed the Wi-Fi's. It is obvious that this is happening due to the data rate being much higher for the Li-Fi subsystem. Moreover, in Fig. 8, it is shown that the power consumption of the Li-Fi AP is similar to the Wi-Fi one, for the lower capacities. This happens despite the fact that Li-Fi is reaching quite higher data rates, since $\alpha = 0.8$. No different than Fig. 7, as soon as the Li-Fi is able to reach much higher speeds, the power consumption of the Li-Fi AP is growing.

V. Conclusion

In this paper, we have investigated a hybrid Li-Fi/Wi-Fi network with the assumption that both subsystems are served by the same backhaul with limited capacity. We have formulated and solved a resource allocation optimization problem, which takes into account the different characteristics of each system. The simulation results illustrate the effectiveness of the proposed technique to fairly distribute the available resources.

References

[1] M. Kavehrad, "Sustainable Energy-Efficient Wireless Applications using Light," *IEEE Commun. Mag.*, vol. 48, no. 12, pp. 66–73, Dec. 2010.

[2] S. Arnon, J. Barry, and G. Karagiannidis, *Advanced Optical Wireless Communication Systems*. Cambridge University Press, 2012.

[3] M. Ayyash, H. Elgala, A. Khreishah, V. Jungnickel, T. Little, S. Shao, M. Rahaim, D. Schulz, J. Hilt, and R. Freund, "Coexistence of WiFi and LiFi toward 5g: Concepts, Opportunities, and Challenges," *IEEE Commun. Mag.*, vol. 54, no. 2, pp. 64–71, Feb. 2016.

[4] M. Uysal, C. Capsoni, Z. Ghassemlooy, A. Boucouvalas, and E. Udvary, *Optical Wireless Communications: An Emerging Technology*. Springer, 2016.

[5] P. D. Diamantoulakis and G. K. Karagiannidis, "Simultaneous Lightwave Information and Power Transfer (SLIPT) for Indoor IoT Applications," in *Proc. IEEE Global Communications Conference*, Dec. 2017, pp. 1–6.

[6] S. Arnon, *Visible light communication*. Cambridge University Press, 2015.

[7] D. Bykhovsky and S. Arnon, "Multiple Access Resource Allocation in Visible Light Communication Systems," *J. Lightwave Technol.*, vol. 32, no. 8, pp. 1594–1600, 2014.

[8] M. S. A. Mossaad, S. Hranilovic, and L. Lampe, "Visible Light Communications Using OFDM and Multiple LEDs," *IEEE Trans. Commun.*, vol. 63, no. 11, pp. 4304–4313, Nov. 2015.

[9] H. Marshoud, V. M. Kapinas, G. K. Karagiannidis, and S. Muhaidat, "Non-Orthogonal Multiple Access for Visible Light Communications," *IEEE Photon. Technol. Lett.*, vol. 28, no. 1, pp. 51–54, Jan. 2016.

[10] X. Li, R. Zhang, and L. Hanzo, "Cooperative Load Balancing in Hybrid Visible Light Communications and WiFi," *IEEE Trans. Commun.*, vol. 63, no. 4, pp. 1319–1329, Apr. 2015.

[11] F. Wang, Z. Wang, C. Qian, L. Dai, and Z. Yang, "Efficient Vertical Handover Scheme for Heterogeneous VLC-RF Systems," *J. Opt. Commun. Netw.*, vol. 7, no. 12, pp. 1172–1180, 2015.

[12] M. Kashef, M. Abdallah, N. Al-Dhahir, and K. Qaraqe, "On the Impact of PLC Backhauling in Multi-User Hybrid VLC/RF Communication Systems," in *2016 EEE Global Communications Conference (GLOBECOM)*, 2016, pp. 1–6.

[13] L. Feng, R. Q. Hu, J. Wang, P. Xu, and Y. Qian, "Applying VLC in 5G Networks: Architectures and Key Technologies," *IEEE Network*, vol. 30, no. 6, pp. 77–83, Nov. 2016.

[14] D. A. Basnayaka and H. Haas, "Design and Analysis of a Hybrid Radio Frequency and Visible Light Communication System," *IEEE Trans. Commun.*, vol. 65, no. 10, pp. 4334–4347, Oct. 2017.

[15] T. Komine and M. Nakagawa, "Fundamental Analysis for Visible-Light Communication System Using LED Lights," *IEEE Trans. Consum. Electron.*, vol. 50, no. 1, pp. 100–107, Feb. 2004.

[16] H. Ma, L. Lampe, and S. Hranilovic, "Coordinated Broadcasting for Multiuser Indoor Visible Light Communication Systems," *IEEE Trans. Commun.*, vol. 63, no. 9, pp. 3313–3324, Sep. 2015.

[17] J. M. Kahn and J. R. Barry, "Wireless Infrared Communications," *Proc. IEEE*, vol. 85, no. 2, pp. 265–298, Feb. 1997.

[18] J. B. Wang, Q. S. Hu, J. Wang, M. Chen, and J. Y. Wang, "Tight Bounds on Channel Capacity for Dimmable Visible Light Communications," *J. Lightw. Technol.*, vol. 31, no. 23, pp. 3771–3779, Dec. 2013.

[19] X. Wu, M. Safari, and H. Haas, "Access Point Selection for Hybrid Li-Fi and Wi-Fi Networks," *IEEE Trans. Commun.*, vol. 65, no. 12, pp. 5375–5385, Dec. 2017.

[20] ——, "Joint Optimisation of Load Balancing and Handover for Hybrid LiFi and WiFi Networks," in *2017 IEEE Wireless Communications and Networking Conference (WCNC)*, Mar. 2017, pp. 1–5.

[21] S. Boyd and L. Vandenberghe, *Convex optimization*. Cambridge university press, 2004.